Special issue of the 3rd International Conference on Computational and Experimental Science and Engineering (ICCESEN 2016)

Numerical Investigation on Hydrodynamic Combustion and NO_x Emission Behavior in 8 MW Circulating Fluidized Bed

O. İpek, B. Gürel and M. Kan
Suleyman Demirel University, Mechanical Engineering Department, Isparta, Turkey

Multi-phase flow is one of the types of flow which is frequently observed in natural phenomena and engineering applications. Circulating fluidized beds constitute an important application of multi-phase flow. The combustion and emission behaviours in circulating fluidized beds are determined by hydrodynamic of bearing. The most appropriate combustion can be provided with the hydrodynamic structure of bearing, taking into account fuel and operating parameters. Therefore, the hydrodynamic structure of circulating fluidized beds should be displayed with mathematical/physical modelling and simulation approach for its analysis and synthesis. Mathematical analysis in today's conditions is very difficult or impossible because of excessive turbulence, unstable and two-phase flow characteristics of the bed. Therefore, the most effective way to do this is the use the physical modelling and simulation approach. In this study, 8 MW circulating fluidized bed hydrodynamic analysis are made by ANSYS-FLUENT R14 commercial CFD code and then combustion and emissions analysis are made with hydrodynamic analysis results. These analysis results show that combustion chamber exit mean NO_x emission was 38.5 ppm and combustion chamber exit mean temperature was 1123 K.

DOI: 10.12693/APhysPolA.132.553
PACS/topics: circulating fluidized bed, hydrodynamic analysis, multi-phase flow, NO_x emissions, clean coal

1. Introduction

Turkish 88% lignite is named low quality lignite and has lower than 8000 kJ/kg calorific value. Circulating fluidized bed boiler (CFBB) system is most convenient and newest clean coal technology for combustion to low calorific value coals that include high moisture and high ash. Coal, bed material, sulphur, and air mix in combustion chamber for CFBB system. Also, NO_x emissions value is low because this value maintained under lower than 1200 K. In addition, high combustion efficiency and fuel flexibility are provided because low-quality lignite combustion process occurs below the fuel ash melting temperature. CFBB is obtained as 4.5 MW/m^2 thermal power, while bubbling fluidized bed is obtained as 1.3 MW/m^2. Additional particles are separated from the flue gas in the cyclone, and are returned in the boiler. As a result, the proportion of unburned carbon particles decreases. Some studies in the literature about CFBB combustion system are indicated as follows.

Gungor and Eskin developed two-dimensional hydrodynamic model for CFBB. They calculated axial and radial voidage distribution, gas and solid phase pressure drop, solid volume fraction in solid phase, and particle dimension distribution with simulation. They compared and validated model results and experimental results on cold flow CFBB system in literature [1].

Dülger, in his Ph.D. Thesis intended to provide an efficient and low emissions combustion in circulating fluidized bed with using specified algorithm. He generated a feedback signal that was obtained by disposed sensors by collecting necessary data from the reactor and the flue gas according to the predetermined algorithm and thus have checked the coal supply motor and air flow fan. He reported that CFBB combustion system does not need additional filter system to keep the specified limit emissions and consequently, he reported this advantage in terms of installation cost, that one of the major factors to the fore other compared combustion systems [2].

Mirek et al. investigated numerically and experimentally that under similar operating conditions air nozzles affect on temperature and NO_x emissions in a large scale fluidized bed boiler. They showed change of the primary air distribution in the lower part of the combustion chamber effect on combustion process strength and temperature distribution along the boiler height [3].

Erbaş et al. in their works experimentally studied the effect of heat transfer within the bed from the wall heating surface. Their study results are stated higher than heat transfer coefficient was obtained when the particle diameter decreased and gas velocity increased [4].

Weng and Plackmeyer, in their works, they compared experimental results and 3D numerical analysis results by Barracuda computational particle fluid dynamics (CPFD) software for the Duisburg circulating fluidized bed boiler. They stated that this study results were very convenient and Barracuda CPFD program will be a very important tool detecting hydrodynamic, temperature and emissions in fluidized bed in the future optimization studies [5].

Pandey and Kumar, in their works, made two three-dimensional analyses of burning in CFB boiler. They have reached temperature, velocity, pressure, and turbulence kinetic energy contours in the boiler for different fluidization velocity. As a result of the studies, they stated that 6 m/s fluidization velocity is more appropriate than 4 m/s and 5 m/s fluidization velocity for fluidized bed combustion [6].

Portrat and Lamire, in their works, present an analytic approach and computational simulations showing that the sequentiality of the domain-general attentional

exhilarating mechanism is responsible for the inconsistency between humans and model. The practice of a computational model based on this solution ensures to be much better suitable to human data. Results are discussed in reference to modern works on the phonological loop as well as in reference to other computational models of short-term memory [7].

Li et al., in their works, regard the candidate target particle set as unnecessary dictionary and the target template as observation signal to decrease the computational involution and improve the real-time performance of target tracking. In addition, to enhance chasing robustness for better adaptation to illumination and occlusion, the density histogram, local binary pattern feature fusion, trivial templates and energy control parameters are also employed in this study. Finally, large simulation experiments under different circumstances show that the recommended method performs better compared with other methods, and the average computation time decreases greatly [8].

Karaçalı, in his work, studies computational fluid dynamics and finite element analysis simulation models were investigated and developed to interpret engineering properties that affect stent functional features. These characteristics are subjection of material properties on blood flow conditions such as structural load, shear-strain rate, radial strength, and wall shear stresses, which need to be scientifically discovered. In this study, computational fluid dynamics model was made to calculate the wall shear stresses and strain distribution in stented vessel transporting blood to heart [9].

Nagy in his computations takes into account the middle-eastern European climate conditions, geothermal gradient, and soil properties as well as the relevant settled EU standards. The equivalent linear heat transfer coefficients, which in this method also include the effects of thermal bridges, happening in various conditions are summarized in a table and can be calculated by new formulae which are also indicated in the paper using condition-dependent constants, the ground floor's heat transfer coefficient, and the length between the floor and ground level [10].

Simanjuntak et al., in their works, made numerical and experimental studies for hydrodynamics in circulating bubbling fluidized bed that was generated internally as cylinder. They have used the FLUENT 6.3 software for CFD simulations in the study that used Eulerian–Eulerian model for solid particle flow. The study noted that, in compliance with the experimental results and simulation results, it was stated that the fluidization in the simulation was affected by flow rate in the flow pipe, air flow rate, initial bed static height, and the orifice diameter [11].

Hydrodynamic, combustion and NO_x analyses of a CFBB system have been done for 8 MW. In this study results showed high circulating efficiency, 1123–1173 K temperature in boiler, 99% carbon combustion efficiency and 38.5 ppm averaged NO_x emissions in boiler exit.

2. Numerical modelling

In this study, combustion and emission features have been investigated in CFBB. In this spirit, before CFBB that, shown in Fig. 1, has been designed with 3D CAD program, then boundary conditions, shown in ANSYS Design Modeler, have been created, and mesh structure that includes 2.000.000 polygonal mesh elements has been created, as shown in Fig. 2.

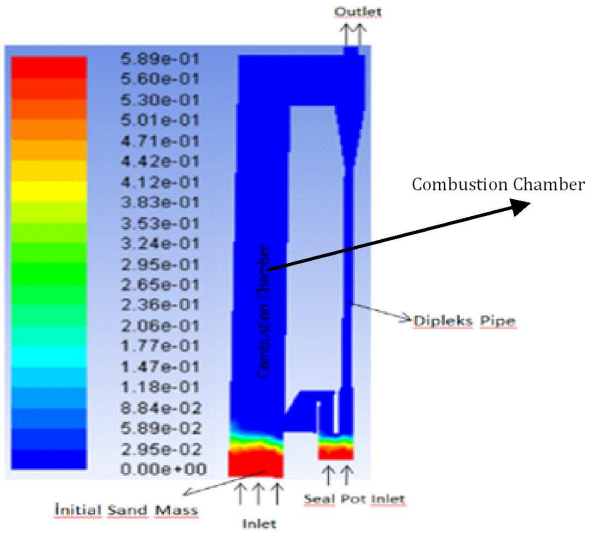

Fig. 1. Boundary conditions of CFB.

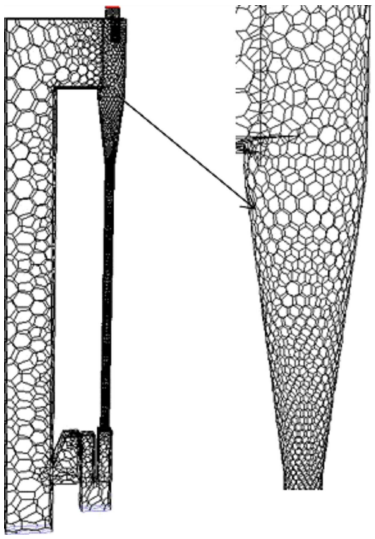

Fig. 2. Mesh of CFB geometry.

Hydrodynamic analysis of CFBB system have been made for 2.1 kg/s primary air flow rate, 1.5 m bed material initial bed height, 0.5 kg/s seal pot air flow rate, and 0.2 m bed material initial bed height.

Realizable k–e turbulence method [12, 13], Eulerian–Eulerian multiphase method [14–16] and the Gibilaro drag coefficient [17] have been used in the numerical analysis. Bed material diameter that was used in the

analysis is 300 μm. Primary air and seal pot air temperature, viscosity and density have been used respectively as 500 K, 2.1×10^{-5} kg/(m s), and 0.6964 kg/m^3 in the hydrodynamic analysis. Initial bed material volume fraction and viscosity have been used respectively as 0.589 [18] and 0.001003 [19, 20]. Realizable k-e turbulence method [12, 13], finite rate-eddy dissipation (FR-ED) volatile combustion model [21, 22], and multiple surface reactions model [21] have been used for modelling char combustion on particle surface. Also, Eulerian–Lagrange discrete phase model [21, 23] and discrete ordinates radiation model [21, 23–26] have been used in combustion analysis. Equations that used hydrodynamic, combustion NO_x emissions analysis in multiphase flow are given in Section 2.1. Primary air temperature, primary air flow rate, secondary air temperature, secondary air flow rate, coal temperature, and coal flow rate have been used respectively as 500 K, 2.1 kg/s, 300 K, 0.7 kg/s, 300 K and 0.36 kg/s in this analysis. Used in the analysis GLİ–Tunçbilek coal elemental and proximate contents are given in Table I.

TABLE I

Elemental and proximate analysis [%] of GLİ–Tunçbilek coals used in analysis.

Coal elemental (ultimate) analysis				
C	H	O	N	S
72.9	5	14.7	2.5	4.9
Proximate analysis				
ash	moisture	volatile matter		fixed carbon
32.6	13	14.8		39.53

2.1. Model equations

Conservation equations that used multiphase flow hydrodynamic, combustion and NO_x emissions analysis are as follows:

Continuity

$$\frac{\partial}{\partial t}\left(\alpha_q\rho_q\right)+\nabla\left(\alpha_q\rho_q\boldsymbol{v}_q\right)=0, \tag{1}$$

$$\alpha_q+\alpha_s=1. \tag{2}$$

Feature equations

$$\frac{\partial}{\partial t}\left(\alpha_q\rho_q X_q^t\right)+\nabla\left(\alpha_q\rho_q X_q^t\right)= \nabla\left(\alpha_q\rho_q D_k^t\nabla X_q^t\right)+S_q. \tag{3}$$

Momentum

$$\frac{\partial}{\partial_t}\left(\alpha_q\rho_g\boldsymbol{v}_q\right)+\nabla\cdot\left(\alpha_q\rho_q v\boldsymbol{v}_q\right)= \nabla\cdot\bar{\bar{\tau}}_q-\alpha_q\nabla+\alpha_q\rho_g\boldsymbol{g}+F_q. \tag{4}$$

Gas phase

$$F_q=K_{qs}(\boldsymbol{v}_s-\boldsymbol{v}_q), \tag{5}$$

$$\bar{\bar{\tau}}_q=\alpha_g\mu_{g,eff}\left(\nabla\boldsymbol{v}_g+\nabla_{\boldsymbol{v}_g}^T\right) +\alpha_g\left(\lambda_g-\frac{2}{3}\mu_g\right)\nabla\boldsymbol{v}_q\bar{\bar{I}}, \tag{6}$$

$$\mu_{g,eff}=\mu_g+\mu_{g,t}. \tag{7}$$

Solid phase

$$F_q=K_{sq}\left(\boldsymbol{v}_q-\boldsymbol{v}_s\right), \tag{8}$$

$$\bar{\bar{\tau}}_s=-P_s\bar{I}+\alpha_s\mu_s\left(\nabla\boldsymbol{v}_s+\nabla\boldsymbol{v}_s^T\right) +\alpha_s\left(\lambda_s-\frac{2}{3}\mu_s\right)\nabla\cdot\boldsymbol{v}_s\bar{\bar{I}}, \tag{9}$$

$$\lambda_s=\frac{4}{3}\alpha_s\rho_s d_s g_{0,ss}\left(1+e_{ss}\right)\left(\frac{\Theta_s}{\pi}\right)^{1/2}. \tag{10}$$

Energy

$$\frac{\partial}{\partial t}\left(\alpha_q\rho_q h_q\right)+\nabla\cdot\left(\alpha_q\rho_q\boldsymbol{v}_q h_q\right)=-\alpha_q\frac{\partial P_q}{\partial t}+\bar{\bar{\tau}}_q:\nabla\boldsymbol{v}_q -\nabla\cdot\boldsymbol{q}_q+Q_{PQ}+S_q, \tag{11}$$

$$Q_{gs}=\frac{6k_g\alpha_g\alpha_s Nu_g}{d_s^2}\left(T_g-T_s\right). \tag{12}$$

Discrete phase model

$$\frac{\mathrm{d}u_p}{\mathrm{d}t}=F_D\left(u-u_p\right)+\frac{g_x(\rho_p-\rho)}{\rho_p}+F_x. \tag{13}$$

Devolatilization carbon combustion model

$$R'=T^\beta A\mathrm{e}^{-E/RT}\left(P_n-\frac{R'}{D'}\right)^N. \tag{14}$$

Combustion reactions

$$Vol+\mathrm{O_2}\rightarrow a\mathrm{CO}+b\mathrm{H_2},$$

$$\mathrm{CO}+\tfrac{1}{2}\mathrm{O_2}\rightarrow\mathrm{CO_2},\ \mathrm{H_2}+\tfrac{1}{2}\mathrm{O_2}\rightarrow\mathrm{H_2O},$$

$$\mathrm{C_s}+\tfrac{1}{2}\mathrm{O_2}\rightarrow\mathrm{CO},\ \mathrm{C_s}+\mathrm{CO_2}\rightarrow 2\mathrm{CO},$$

$$C_s+H_2O\rightarrow H_2+CO.$$

NO_x modelling, thermal NO_x Zeldovich mechanisms reactions [19, 27]:

$$\mathrm{O}+\mathrm{N_2}\rightarrow\mathrm{NO}+\mathrm{N},\ \mathrm{N}+\mathrm{NO}\rightarrow\mathrm{N_2}+\mathrm{O}$$

$$\mathrm{N}+\mathrm{O_2}\rightarrow\mathrm{NO}+\mathrm{O},\ \mathrm{O}+\mathrm{NO}\rightarrow\mathrm{O_2}+\mathrm{N},$$

$$N+OH\rightarrow NO+H,\ H+NO\rightarrow OH+N.$$

3. Results and discussions

Hydrodynamic analysis results are given in Fig. 3.

As could be seen in Fig. 3, sand volume fraction in CFB furnace did not change after 200 s from start up conditions. In this analysis results, sand volume fraction was respectively 5–8% in combustion chamber, 6–9% in dip-leg pipe, and 15–18% in loop-seal.

As could be seen in Fig. 4, air velocity in CFB furnace did not change after 200 s from start up conditions. In this analysis results, air velocity was respectively 5–7.5 m/s in combustion chamber and cyclone, 15–17.5 m/s in dip-leg pipe, and 0.2–5 m/s in loop-seal.

As could be seen in Fig. 5, sand velocity in CFB furnace did not change after 200 s from start up conditions. In this analysis results sand velocity was respectively 3–

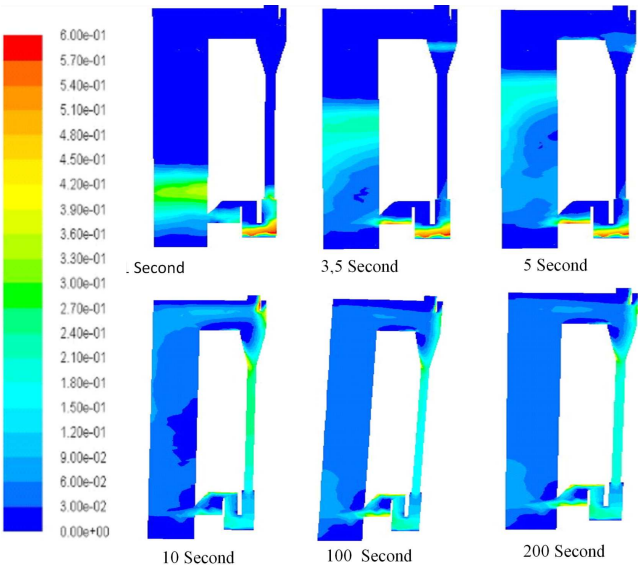

Fig. 3. Changing of temporal sand volume fraction in solid circulating system.

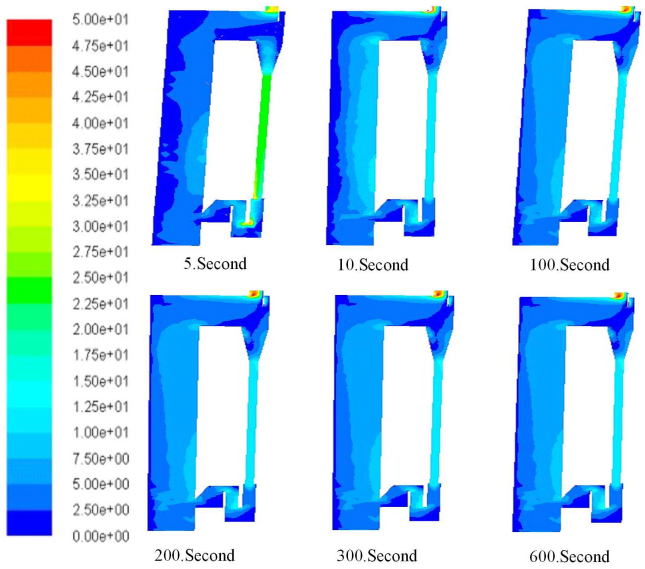

Fig. 4. Changing of temporal air velocity in solid circulating system.

5 m/s in combustion chamber, 5–6 m/s in cyclone, 12–15 m/s in dip-leg pipe, and 0–3 m/s in loop seal.

As could be seen from Fig. 4, air velocity in combustion chamber is 6 m/s for steady-state conditions. Also, sand velocity in combustion chamber is 4 m/s. 2.8 kg/s air is used for combustion of 0.36 kg/s Tunçbilek lignite at 1.2 stoichiometric rate [28]. Primary air mass flow rate is 2.1 kg/s and 500 K and secondary air mass flow rate is 0.7 kg/s and 300 K. This secondary air is added at 6 m height from combustion chamber base. These conditions are given in Fig. 6. In this analysis, non-premixed combustion and discrete phase method are used for relatively coal combustion and injection of coal in combustion chamber. Also, the Zeldovich mechanisms [29], the

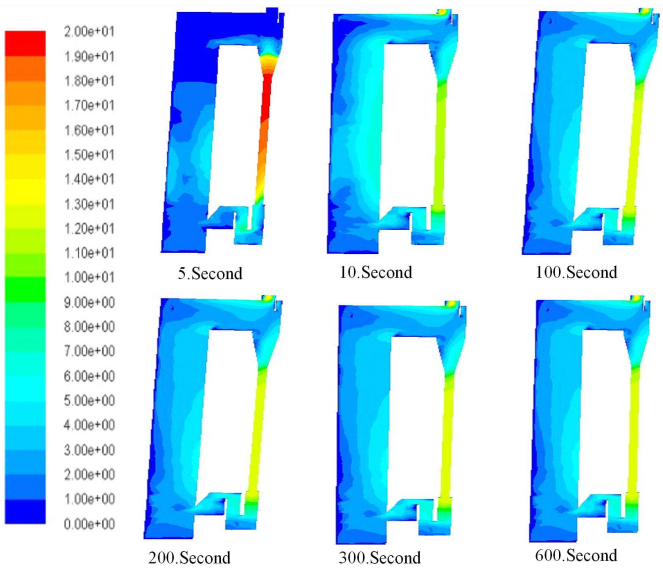

Fig. 5. Changing of temporal sand velocity in solid circulating system.

De-Seote global reaction kinetics [30] and equivalence ratio 1/1.2 are used for calculations of relatively thermal NO_x formation, via fuel NO_x formation and prompt NO_x formation in the combustion chamber.

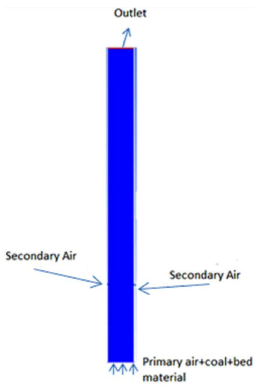

Fig. 6. CFBB combustion chamber boundary conditions.

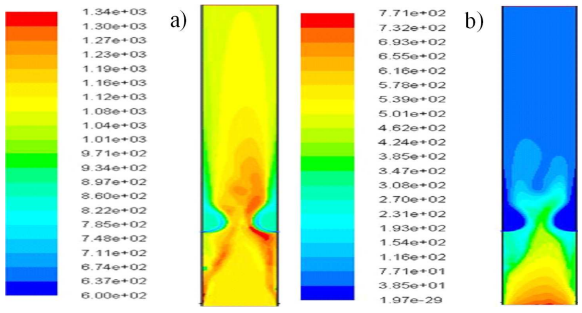

Fig. 7. Combustion chamber: (a) temperature [K], (b) NO_x [ppm] emissions distribution.

Temperature and NO_x emissions distribution are given in Fig. 7. As could be seen in Fig. 7, NO_xemission rose

to 771 ppm and this was reduced through in combustion chamber. NO_x emissions was reduced to 38.5 ppm and stationary these conditions and combustion chamber exit temperature was 1123 K. Hydrodynamic and combustion analysis results and referee studies [18, 26, 31, 32] results are convenient with each other.

4. Conclusions

Circulating fluidized bed processing is known as most clean and efficiency coal combustion technologies. In this study, GLİ–Tunçbilek coal which contains high moisture and ash, combustion and hydrodynamic characteristic was investigated in 8 MW circulating fluidized bed combustor. Air combustion chamber inlet and combustion chamber mean velocity was observed as 6 m/s and this velocity was used in combustion and NO_x emission analysis. These analysis results revealed that circulating fluidized bed combustors are most convenient combustors for low quality (8000 kJ/kg) Turkish lignites. In next studies, oxy-fuel combustion, staged secondary air, and solar energy assisted innovations will be included in CFBC combustion process and will investigate temperature and NO_x, SO_x emissions results in developed process.

References

[1] A. Güngör, N. Eskin, *Tesisat Mühendisliği Dergisi* **84**, 7 (2004).

[2] S. Dülger, Ph.D. Thesis, Ankara 2008.

[3] P. Mirek, R. Sekret, W. Nowak, in: *Proc. Fluidization XII, New Horizons in Fluidization Engineering*, Vancouver 2007, p. 969.

[4] O. Erbaş, H. Topal, A. Durmaz, *Dumlupınar Üniversitesi Fen Bilimleri Enstitüsü Dergisi* **16** 91 (2008), (in Turkish).

[5] M. Weng, J. Plackmeyer, in: *Proc. 10th Int. Conf. on Circulating Fluidized Beds and Fluidization Technology — CFB-10*, 2011, Ed. T.M. Knowlton, p. 545.

[6] K.M. Pandey, R. Kumar, *Int. J. Chem. Eng. Appl.* **2**, 5 (2011).

[7] S. Portrat, B. Lemire, *Cognit. Comput.* **7**, 333 (2015).

[8] G. Li, Z.Y. Liu, Hou-Biao Li, P. Ren, *Cognit. Comput.* **8**, 910 (2016).

[9] Ö. Karaçalı, *Acta Phys. Pol. A* **130**, 249 (2016).

[10] B. Nagy, *Acta Phys. Pol. A* **128**, B-164 (2015).

[11] J.P. Simanjuntak, Z.A. Zainal, M.Z. Abdullah, *Int. J. Renew. Energy Biofuels* , 993061 (2014).

[12] M. Gharebaghi, R.M.A. Irons, L. Ma, M. Pourkashanian, A. Pranzitelli, *Int. J. Greenhouse Gas Contr.* **5S**, S100 (2011).

[13] P. Stopford, *Appl. Math. Modell.***26**, 351 (2002).

[14] Y. Jiang, G. Qiu, H. Wang, *Chem. Eng. Sci.* **109**, 85 (2014).

[15] H. Liu, A. Elkamel, A. Lohi, M. Biglari, *Ind. Eng. Chem. Res.* **52**, 18162 (2013).

[16] J. Xie, W. Zhong, B. Jin, Y. Shao, H. Liu, *Energy Fuels* **28**, 5523 (2014).

[17] L.G. Gibilaro, R. Di Felice, S.P. Waldram, *Chem. Eng. Sci.* **40**, 1817 (1985).

[18] Ö. Baysal, M.Sc. Thesis, Gazi University, 2007.

[19] *ANSYS FLUENT 14 User Guide*, Fluent Inc., USA 2013.

[20] F. Kumaş, M.Sc. Thesis, Dumlupınar University, Kütahya 2009.

[21] B. Gurel, O. Ipek, M. Kan, *Acta Phys. Pol. A* **128**, B-43 (2015).

[22] P. Warzecha, A. Boguslawski, *Energy* **66**, 732 (2014).

[23] R. Jovanovic, A. Milewska, B. Swiatkowski, A. Goanta, H. Spliethoff, *Int. J. Heat Mass Transf.* **54**, 921 (2011).

[24] R. Backreedy, L. Fletcher, L. Ma, M. Pourkashanian, A. Williams, *Combust. Sci. Technol.* **178**, 763 (2006).

[25] E.H. Chui, G.D. Raithby, *Num. Heat Transf. Part B* **23**, 269 (1993).

[26] G.D. Raithby, E.H. Chui, *J. Heat Transfer* **112**, 415 (1990).

[27] J.B. Heywood, *Internal Combustion Engine Fundamentals*, McGraw-Hill, Singapore 1988, p. 336.

[28] Y. Chang, K. Wu, Y. Chen, C. Chen, *Energy Fuels* **29**, 3476 (2015).

[29] S. Belosevic, I. Tomanovic, V. Beljanski, D. Tucakovic, T. Zivanovic, *Appl. Therm. Eng.* **74**, 102 (2015).

[30] G.G. De Soete, *Proc. Combust. Inst.* **15**, 1093 (1975).

[31] A.E. Atımtay, H. Olgun, U. Kayahan, A. Ünlü, B. Engin, M. Varol, M. Çömlekçioğlu, B. Kamalı, H. Atakül, G. Bardakçıoğlu, *Biores. Techn.* **224** (C), 601 (2011).

[32] M. Varol, A.T. Atimtay, H. . Olgun, *Fuel* **130**, 1 (2014).